RESEARCH

Enhanced vibration measurement through frequency modulated laser diode self-mixing interferometry

Jiung-Ran Liao[1] · Jian-Ming Cheng[1] · Vincent K.S. Hsiao[1]

Abstract

Self-mixing interference (SMI) has emerged as a powerful non-contact vibration sensing technique, leveraging the inherent coupling between laser emission and external optical feedback. However, conventional SMI systems often face limitations in signal resolution and measurement accuracy, particularly when probing low-amplitude vibrations or low-reflectivity targets. This study proposes a frequency modulation (FM) approach, FM-SMI, to enhance the capabilities of SMI setups. By intentionally modulating the laser frequency of 20 kHz, the FM-SMI technique induces a segmentation of the interference signal, effectively increasing the temporal resolution and facilitating the detection of finer vibration details. Comprehensive experiments involving oscillating speakers and rotating silicon wafers validate the superior performance of the FM-SMI system. Notably, the frequency-modulated signals exhibit stability and robustness, even under low-amplitude vibration conditions or when targeting low-reflectivity surfaces. The enhanced signal quality, coupled with numerical processing techniques, enables precise extraction of vibration characteristics, including amplitude variations and surface topographies. The proposed FM-SMI approach demonstrates its potential as a versatile tool for high-precision, non-contact vibration measurements across diverse applications, such as, non-destructive testing and the characterization of vibration induced by the rotational systems.

1 Introduction

Laser interferometry has been a sensing technique in industrial and laboratory settings for over half a century, enabling precise measurements of displacement, velocity, vibration, and distance [1–3]. Traditional interferometric methods, such as the Michelson and Mach-Zehnder interferometers [4–6], rely on complex external setups with mirrors, prisms, and lenses. However, a new paradigm emerged with the development of self-mixing interferometry (SMI) [7–12], a technique that utilizes the feedback effect within the laser cavity itself. The intriguing phenomenon of self-mixing interference SMI using semiconductor laser diode (LD) was first investigated in the field [13]. SMI occurs when a portion of the light emitted by a LD is reflected back into the laser cavity by an external target [14]. The re-injected light,

carrying the vibration dynamics information from the target, interacts with the intracavity light within the laser diode cavity, resulting in modulation of the laser's output power [15]. This modulated optical output is subsequently detected by the integrated photodiode (PD) within the LD structure [16]. Unlike conventional interferometry based on interference between two independent beams split from a common source, SMI involves interference between the intracavity light and the re-entering reflected light within the laser cavity itself. Interestingly, SMI has been observed even when the external target is positioned far beyond the coherence length of the laser source [17]. This implies the interference effect is not dependent on the temporal coherence of the laser. Additionally, SMI appears independent of whether the laser operates in single-mode or multimode regimes, as well as the type of fiber used to couple the laser to the target. Later, a SMI vibrometer was developed, relying on locking the system to half the interferometric fringe and employing active phase-nulling via wavelength modulation [18]. This allows an extended dynamic range to be achieved while maintaining good sensitivity to sub-wavelength vibrations. A prototype SMI vibrometer has been designed and constructed that can operate on nearly any type of rough

✉ Vincent K.S. Hsiao
  kshsiao@ncnu.edu.tw

1   Department of Applied Materials and Optoelectronic
    Engineering, National Chi Nan University, Nantou
    54561, Taiwan

surface, covering the vibration frequency range from 0.1 Hz to 70 kHz [14]. The proposed SMI laser vibrometer method opens up applications in modal analysis as well as noise and vibration measurement in industrial and scientific environments. The key advantages over traditional approaches are the greatly simplified setup enabled by the self-mixing configuration and the ability to achieve high sensitivity and dynamic range simultaneously. For example, the SMI method has been developed for determining sub-micron particle sizes as well as measuring flows in narrow diameter tubes [19–21]. The rate equations governing LDs subjected to frequency-shifted optical feedback are examined and extended to include a normalized frequency distribution that can be characterized by the backscattered light spectrum. Experimental investigations shown the precisely determining the particle sizing of polystyrene particles in water ranging from 0.02 to 0.20 μm in diameter using SMI. The observed frequency band increases for smaller particles when observing Brownian motion, and for higher flow rates when observing flowing liquids.

The SMI effect in LDs could also be employed as a simple translation technique to measure the optical phase shift as a function of the moving distance of the sample [22]. The refractive index could be determined by analyzing the fringe number of the SMI signals with respect to the sample's moving distance and the angle of incidence [23]. An experimental accuracy of 0.004 is achieved. Interestingly, the measurement error of the proposed SMI system can be effectively reduced by modifying the angle of incidence. This method also shows the advantage of enabling measurement over a large range of refractive index values. Since the SMI method utilizes a simple LD, interference is detected within the laser cavity itself and measured as optical power fluctuations by the integrated PD. This allows SMI to combine the advantages of high resolution point displacement sensing with a highly compact and easy to operate configuration. For proper adaptation of SMI to monitor ablation depth in laser micromachining processes, certain optical, electronic, and mechanical limitations need to be overcome [24]. In laser surface texturing of thin ceramic coatings, precise control of ablation depth is critically important to avoid substrate contamination damage. SMI was applied to monitor the laser percussion drilling of 4 μm thick TiN coatings using a 1 ns green fiber laser, while a 785 nm laser diode enabled the SMI monitoring. In their works, the SMI measurements were compared to a conventional optical measurement device. The SMI concept was successfully validated, as the measurements were statistically equivalent between the two methods. Recent works have proposed using SMI as a promising non-destructive sensing method employed for measuring the Young's moduli and internal frictions by detecting the resonance frequencies and damping factors

of specimen vibrations induced by impulse excitation [25]. Simulations and experiments were carried out to verify the feasibility of the proposed fringeless SMI method. Specimens of brass and aluminum were tested. The experimental results showed standard deviations of Young's moduli were 0.20 GPa for brass and 0.14 GPa for aluminum. The standard deviations of internal friction were 4.0×10^{-5} for brass and 5.4×10^{-5} for aluminum. Recent advancements in SMI technology have led to the development of a time-multiplexed fiber-coupled laser SMI sensor integrated with impulse excitation technique. This innovative approach enables simultaneous measurement of Young's modulus, shear modulus, and Poisson's ratio of materials, demonstrating the expanding capabilities of SMI in comprehensive assessment of material mechanical properties [26].

Traditional SMI techniques have primarily focused on detecting amplitude modulation (AM) signals, limiting their sensitivity and dynamic range. Advancements have explored the use of frequency modulation (FM) signals, which offer higher signal-to-noise ratios but present challenges in detection [27–31]. The key advantages of this emerging trend in laser interferometry include an extremely high sensitivity to scattered light, the ability to estimate displacement direction and obtain information from small object surface areas, simple interferometer design, and low implementation cost [32, 33]. The main aspects highlighted are the operating principles based on optical feedback and frequency modulation of laser diodes, analysis of the interference signals for various measurement applications, establishing relationships between object motion and signal parameters, and the significant advantages offered by this approach in terms of scattered light sensitivity, directionality information, simplicity, and low cost. A method for reading the FM of a laser diode self-mixing interferometer (LD-SMI) has been developed using a Mach–Zehnder interferometer [30]. This approach offers improved performance compared to the conventional AM signal. The converted FM signal exhibits significantly higher magnitude and better signal-to-noise ratio than the typical AM signal. By employing all-fiber technology to construct the compact Mach–Zehnder filter, which has enhanced the minimum detectable signal of the SMI by a factor of 150. In a LD-SMI setup, the measurement of external reflector displacement usually entails observing the optical-phase signal, which manifests as an AM of the emitted power. Conversely, the signal representing a FM of the emitted field at the optical frequency is often overlooked due to the challenges associated with its recovery. Recent work successfully employed a narrow-band acetylene cell to convert the FM signal into an amplitude signal, revealing that the converted FM signal is not only larger but also exhibits a superior signal-to-noise ratio compared to the AM signal [32]. A straightforward method for determining

the phase shift between the AM and FM of a LD was also demonstrated. The approach involves measuring the AM and FM signals generated by the dynamic response of a laser diode under weak optical feedback. The AM signal is directly measured using a photodiode to detect the emitted power, while the FM signal is converted to intensity modulation through edge-filtering techniques employing either a volumetric Bragg grating or a Mach-Zehnder interferometer as filters before signal detection. A new method for measuring multiple-dimensional displacement is presented, which combines SMI with frequency division multiplexing (FDM) [34]. This technique involves using a single laser to produce three modulated light beams, each with a distinct carrier frequency. These beams are directed onto a planar grating, each at its unique auto-collimation diffraction angle, before being reflected back to the laser cavity. Inside the cavity, self-mixing interference occurs. An algorithm based on FDM is then employed to reconstruct the multiple-dimensional displacement from a single SMI signal, extracting information from the different modulated beams. Experimental results validate the effectiveness of this approach, highlighting its compact configuration, high resolution, and improved immunity to environmental disturbances. These qualities make it an attractive option for applications requiring precise and reliable multiple-dimensional displacement sensing.

In this study, we present an approach to enhance the capabilities of SMI systems by implementing frequency modulation of the laser beam. Our findings demonstrate that the proposed FM-SMI technique offers significant advantages over conventional unmodulated SMI setups. The frequency modulation of the laser beam results in a segmentation of the interference signal into higher-resolution components, effectively increasing the temporal sampling rate and enabling the detection of finer vibration details. Remarkably, the FM-SMI approach exhibits exceptional signal stability and robustness, even when targeting low-reflectivity surfaces or probing minute vibration amplitudes. Through comprehensive experimental investigations involving oscillating speakers and rotating silicon wafers, we validate the efficacy of our FM-SMI system in accurately characterizing vibration dynamics across a wide range of amplitudes and frequencies. The ability to resolve intricate surface topographies and minute undulations, facilitated by the enhanced signal resolution and numerical processing techniques, positions our FM-SMI technique as a powerful tool for diverse applications demanding high-precision, non-contact vibration measurements.

2 Experimental setup

The experimental setup comprised a commercially available LD integrated with a PD for optical feedback detection. Two driving circuits were employed to modulate the LD, a DC bias combined with a current driver, and an AC voltage source operating at 20 kHz. The emitted laser beam was focused onto the target sample using a lens. Figure 1a illustrates the configuration where a speaker diaphragm served as the vibrating target. A functional generator controlled the frequency and amplitude of the speaker's oscillations, enabling precise modulation of the induced vibrations. The laser light reflected from the oscillating diaphragm underwent self-mixing interference within the LD cavity, and the resulting intensity modulations were detected by the integrated PD. These interference signals were captured using an oscilloscope for subsequent analysis. In a separate experimental setup, depicted in Fig. 1b, a silicon wafer mounted on a spin coater acted as the target reflective surface. The laser beam was focused onto the spinning wafer, and the reflected light carrying the surface dynamics information was self-mixed within the LD cavity, generating interference signals proportional to the wafer's vibrations and topographical undulations. Two distinct driving circuits were employed to modulate the LD's operating conditions. A constant DC bias voltage was applied to the LD, in conjunction with a current driver that controlled the injection current, enabling precise adjustment of the LD's output power. The laser diode was driven with a sinusoidal modulation current at a frequency of 20 kHz, superimposed on a DC bias current of 60 mA. The modulation depth was set to 15 mA peak-to-peak. This current modulation resulted in a corresponding optical frequency modulation of the laser output. This frequency modulation scheme facilitated the segmentation of the self-mixing interference signal into higher-resolution components, enhancing the detection sensitivity and resolution. The combination of these driving circuits allowed for comprehensive investigations into the self-mixing interference phenomena under both unmodulated and frequency-modulated conditions, enabling comparative analyses and the evaluation of the proposed frequency modulation approach's performance.

Figure 2 presents a photograph of the actual experimental setup utilized in this study. A custom-designed 3D-printed socket was employed to facilitate the secure mounting and integration of the LD. This socket provided a convenient platform for electrical connections and optical alignment. The driving circuits responsible for modulating the LD's operation were also incorporated into the setup. These included the direct current DC bias and current driver circuit, as well as the 20 kHz alternating AC voltage source for frequency modulation of the laser beam. For
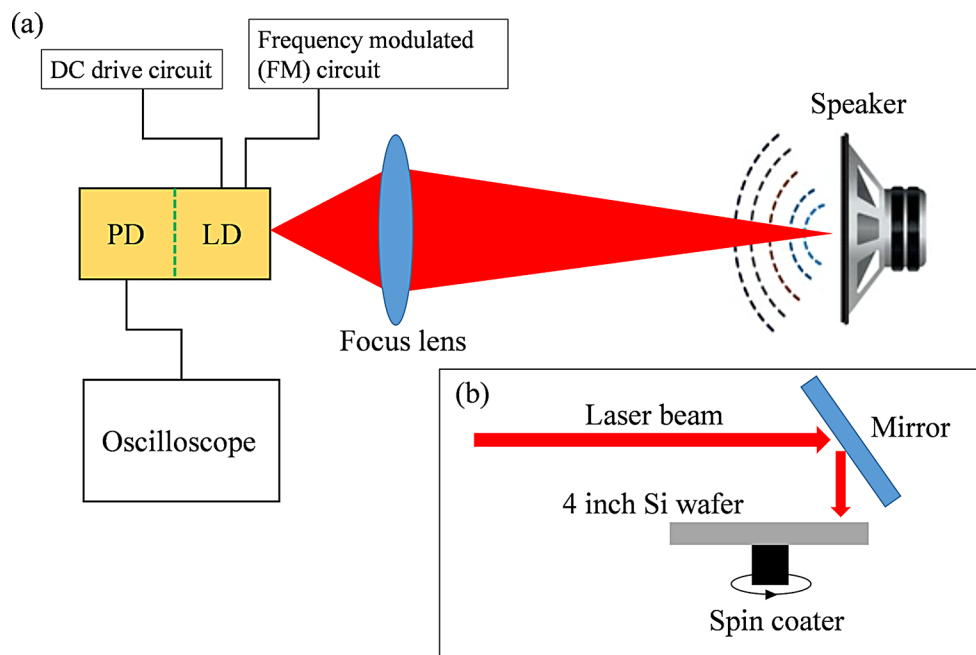
Fig. 1 Schematic illustrations of the experimental setups for self-mixing interference measurements. (**a**) Configuration utilizing a speaker diaphragm as the vibrating target. The laser beam is focused onto the speaker surface, and the reflected light undergoes self-mixing interference within the laser diode cavity. The interference signal, modulated by the speaker's oscillations, is detected by the integrated photodiode. A functional generator controls the frequency and amplitude of the speaker's vibrations. (**b**) Configuration with a silicon wafer mounted on a spin coater serving as the reflective target. The laser beam is focused onto the spinning wafer, and the reflected light, carrying the wafer's surface dynamics, self-mixes within the laser diode cavity, generating interference signals proportional to the wafer's vibrations and topographical undulations
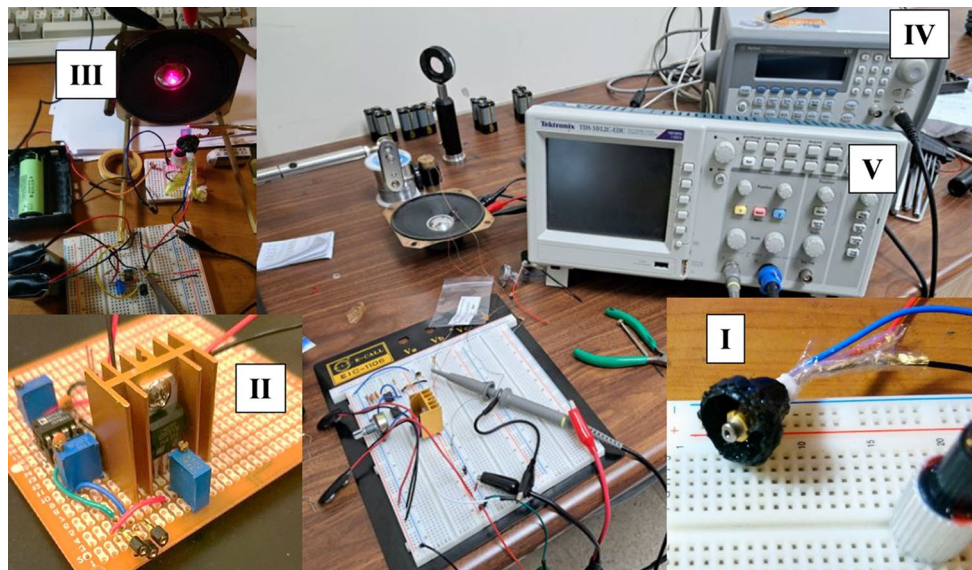

Fig. 2 Photograph of the experimental setup for self-mixing interference measurements. The custom-designed 3D-printed socket (**I**) securely holds the LD and facilitates electrical connections and optical alignment. The driving circuits, comprising a DC bias and current driver, as well as a 20 kHz alternating AC voltage source for frequency modulation, are integrated into the system (**II**). A speaker serves as the vibrating target (**III**), with its oscillation frequency and amplitude controlled by a function generator (**IV**). The emitted laser beam is focused onto the speaker diaphragm, and the reflected light undergoes self-mixing interference within the LD cavity, generating modulated signals detected by the integrated photodiode connected with an oscilloscope (**V**)

the vibration target, a speaker was utilized, as shown in the photograph. The speaker diaphragm served as a reflective surface, enabling the self-mixing interference between the emitted and reflected laser beams. The speaker's oscillation frequency and amplitude were precisely controlled using a function generator, allowing for systematic investigations of the self-mixing interference phenomena under various vibration conditions. The 3D-printed socket, designed specifically for this experiment, played a crucial role in ensuring proper alignment and stability of the LD, while also providing a robust electrical interface for the driving circuits. This custom-made component contributed to the overall reliability and reproducibility of the experimental results.

3 Results and discussion

The operating principle of the SMI system is based on the scattering of laser light from the target object, where the scattered light re-enters the laser cavity. In this process, the laser serves dual roles as a coherent heterodyne receiver and signal amplifier, while simultaneously performing quadratic detection of the recorded signal internally. The behavior of the system can be described as treating the target as an additional mirror in the laser system, forming a three-mirror laser configuration. In this case, the laser possesses an external cavity with a length equal to the distance between the laser and the target, often referred to as the theory of equivalent lens cavities. From this viewpoint, the SMI system can be described by a set of field and rate equations derived by incorporating an external feedback term into the standard laser equations. Alternatively, the system can be viewed as a two-mirror laser with a modified complex reflection coefficient or effective reflection coefficient. In this approach, the solution is obtained by replacing the parameters without feedback with parameters that account for the presence of an additional mirror (the target) in the laser system. Under steady-state operation of the LD, the optical emitting power of an LD with sinusoidal feedback, P, can be expressed as a function of the optical power without the feedback, P_0, as:

$$\mathrm{P} = P_0 \left[1 + m \cdot \cos\left(2\pi\, v \tau_D\right)\right] \tag{1}$$

,Where m is a modulation parameter, v is the frequency of laser light, optical frequency shift, τ_D, is the propagation time between LD and the feedback [16]. The traveling distance of D between LD and the target (external cavity) could be expressed as:

$$\mathrm{D} = D_0 + A_0 \cos\left(2\pi \frac{t}{T}\right) \tag{2}$$

Where T is the oscillation period of the speaker, A_0 is the amplitude due to the vibration of the speaker, and D_0 is the mean position between the LD and the speaker [16]. These variations of P are due to the modulation of the speaker, which changes the optical path length of the equivalent cavity. To extract the amplitude from the experimentally measured LD power signal, a practical approach that leverages the periodic symmetry of the waveform can be employed. Specifically, the number of peaks n_p between two consecutive symmetrical points of the signal can be counted. By doing so, the amplitude can be estimated without the need to directly solve the complex analytical expression given in Eq. (3).

$$A_0 = \frac{n_p \lambda}{4} \tag{3}$$

λ is the wavelength of laser light. This peak-counting method circumvents the requirement of deriving the amplitude from the theoretical formula, providing a convenient approximation technique applicable directly to experimental data. It facilitates the analysis and estimation of the oscillation amplitude of the laser diode emitted power P from the measured signal waveform. To investigate the SMI phenomenon and its application in vibration sensing, experiments were conducted by detecting the SMI signal from a speaker undergoing periodic oscillations at 250 Hz. Figure 3 illustrates the obtained SMI signal waveform under these conditions. Analysis of the signal revealed that during consecutive oscillation cycles, the number of peaks n_p observed between symmetrical points was 8. Leveraging the peak-counting technique described previously, the amplitude of the oscillatory displacement could be estimated from this value of n_p without resorting to complex theoretical derivations. The laser wavelength employed in the experiment was 650 nm. Based on this wavelength and the observed number of peaks $n_p = 8$ over an oscillation period at 250 Hz, a simple calculation indicates that the periodic displacement induced by the speaker vibration was approximately 1.3 μm.

The SMI signal obtained from our experimental setup was analyzed to estimate the feedback parameter C [35, 36], which is crucial for understanding the system's behavior. The observed SMI waveform exhibited characteristics typical of the moderate feedback regime, including asymmetry in the signal shape and slight hysteresis effects, particularly evident in the regions of higher amplitude oscillations. Based on a detailed analysis of the signal morphology [15], we estimated the C value to be in the range of 2.5 to 4. This range is consistent with the moderate feedback regime described in the previous reported data [15], where the SMI signal transitions from a simple sinusoidal shape to a more complex sawtooth-like waveform with increasing
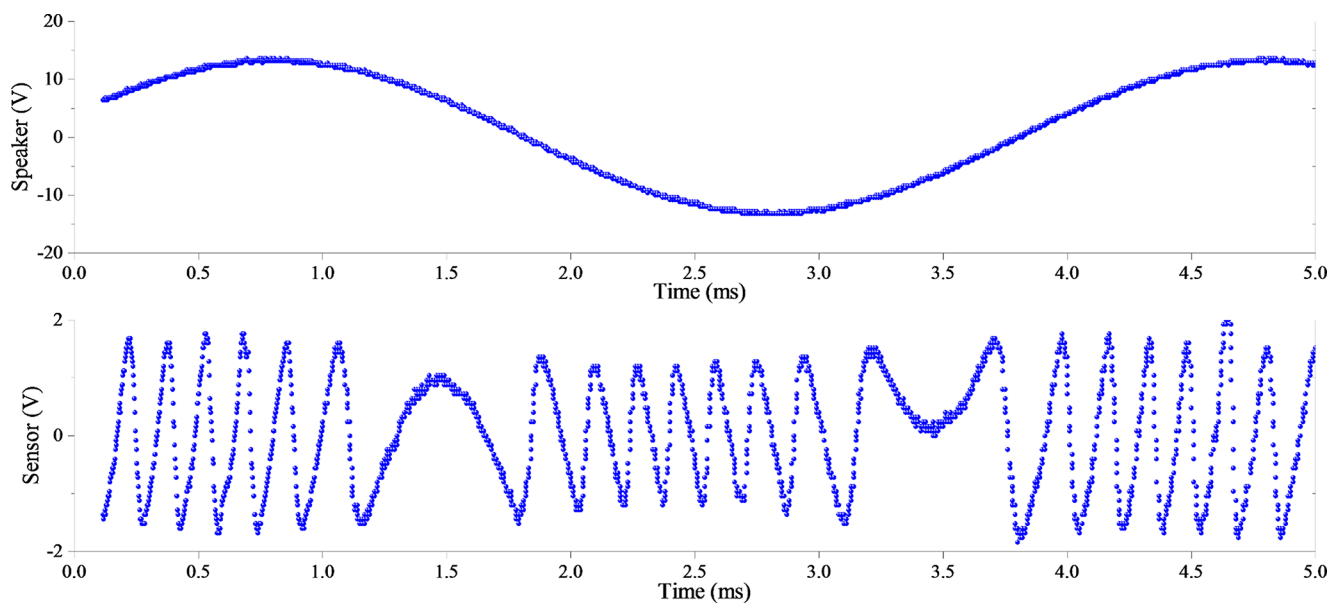
Fig. 3 SMI signal waveform (bellow) obtained from a speaker undergoing periodic oscillations at 250 Hz (above). The number of peaks (n_p) observed between consecutive symmetrical points of the signal is 8, enabling the estimation of the oscillation amplitude using the peak-counting method without resorting to complex theoretical derivations

feedback strength. To corroborate our experimental findings, we employed the theoretical model [15], which relates the C parameter to various system characteristics. Using typical values for a semiconductor laser ($\alpha \approx 5$, $r^2 \approx 0.32$) and estimating other parameters based on our experimental setup, we performed an inverse calculation to determine the system parameters that would yield a C value within our experimentally estimated range. This analysis suggested an external cavity length of approximately 0.5 m and a remarkably low power reflectivity ratio (R/R₀) of about 1.1×10^{-6}. The convergence of our experimental observations and theoretical calculations provides strong support for the validity of our C value estimation. The low reflectivity ratio aligns well with practical considerations in SMI systems, where only a small fraction of the emitted light typically returns to the laser cavity due to factors such as beam divergence and non-ideal target surfaces.

Since the frequency from Eq. (1) is directly related to the speaker vibration distance, we can easily put the relation, $v = c/\lambda$, and Eq. (2) into Eq. (1) and obtain.

$$P = P_0 \left[1 + m \cdot cos\left(4\pi \frac{D_0}{\lambda} + 4\pi \frac{A_0}{\lambda} cos\left(2\pi \frac{t}{T} \right) \right) \right] \quad (4)$$

Equation (4) indicates that optical power (P) from laser light oscillates periodically with time and the modulation frequency determined by the cavity length changes induced by the presence of the speaker. The optical signal captured from the photodetectors exhibited the expected modulation behavior as predicted by theory, under the assumptions of a linear PD response and negligible signal distortion. The measured voltage signal V from oscilloscope was directly proportional to the optical power detected from PD.

$$V = V_0 \left[1 + m \cdot cos\left(4\pi \frac{D_0}{\lambda} + 4\pi \frac{A_0}{\lambda} cos\left(2\pi \frac{t}{T} \right) \right) \right] \quad (5)$$

To validate the reliability of our SMI setup, we substituted the experimental data into the Eq. (4). The calculated results, as shown in Fig. 4, showed excellent agreement with our experimental findings, thereby confirming the robustness of our experimental system. This close correspondence substantiates the credibility of our SMI setup, granting us confidence to proceed with subsequent experiments on this platform.

Departing from the approach employed in Fig. 3, where the focus was on larger speaker amplitudes, we conducted measurements to detect smaller amplitude vibrations induced by the speaker. A function generator was utilized to produce sinusoidal waveforms of varying frequencies to drive the speaker. The resulting displacements corresponding to these smaller amplitude oscillations are depicted in Fig. 5. Our SMI setup successfully captured these minute vibrations, further showing its sensitivity and versatility. The ability to detect minuscule speaker vibrations, as demonstrated in Fig. 5, highlights the remarkable responsiveness of our self-mixing interference apparatus. By employing a function generator to excite the speaker with sinusoidal waves of varying frequencies, we could meticulously control the amplitude of the induced oscillations. This approach
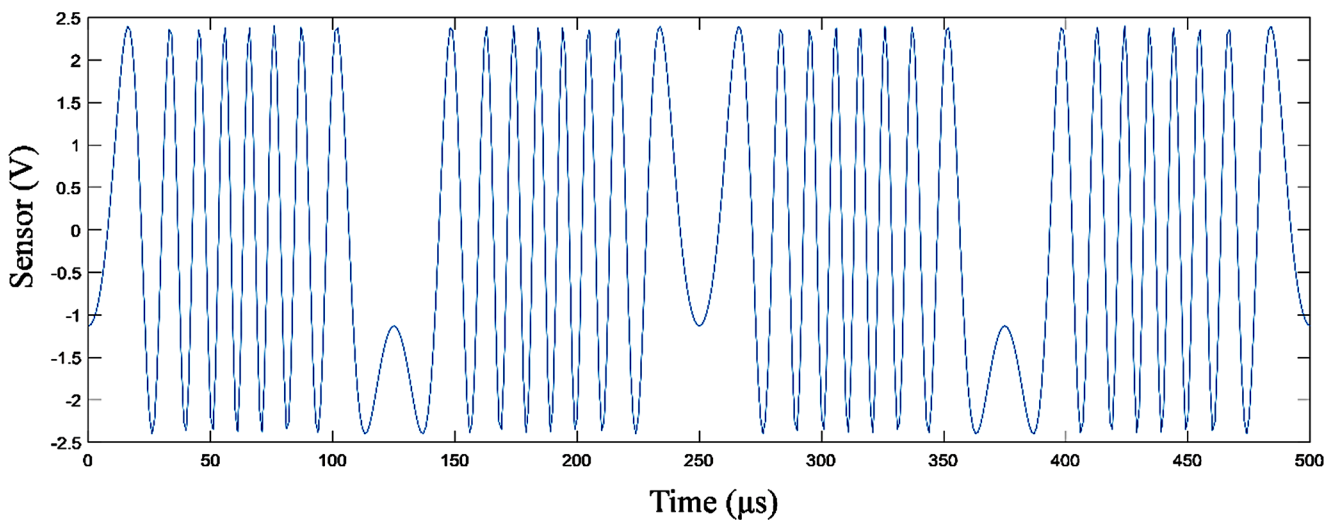
Fig. 4 Calculated optical power modulation resulting from the speaker vibrations, based on substituting the experimental data into the theoretical model (Eq. 4). The excellent agreement with the experimental findings validates the reliability of the SMI experimental setup

diverged from the previously adopted method of using higher amplitude pulse excitations (Fig. 3), allowing us to explore the lower limits of our system's detection capabilities systematically. The excellent agreement between the measured displacements and the controlled input amplitudes substantiates the linear response of our setup across a wide dynamic range. This linearity, coupled with the high sensitivity exhibited in detecting minute vibrations, underscores the robustness and reliability of our SMI technique. These attributes render our experimental platform well-suited for applications demanding precise measurements of oscillatory phenomena, encompassing both large and small amplitude regimes.

To further enhance the capabilities of our SMI setup, we implemented a circuit design that enabled frequency modulation of the laser beam up to 20 kHz. Figure 6 presents a comparative analysis between the SMI signals obtained with the unmodulated laser beam (Fig. 6a) and the frequency-modulated laser beam (Fig. 6b). The frequency modulation clearly resulted in a segmentation of the SMI signal into smaller units, effectively increasing the resolution of the captured vibration patterns. Through subsequent digital filtering and numerical processing techniques, we could extract an improved feedback response from the frequency-modulated SMI signal (Fig. 6c) compared to the unmodulated case. This enhancement in the output signal quality underscores the advantages introduced by our frequency modulation approach. The frequency modulation of the laser beam up to 20 kHz, as illustrated in Fig. 6b, represents a pivotal advancement in our SMI experimental framework. By intentionally modulating the laser frequency, we could subdivide the intrinsic interference patterns typically observed in SMI setups (Fig. 6a) into higher-resolution constituents. This frequency-modulated segmentation of the

SMI signal effectively mimics an increase in the temporal sampling rate, thereby allowing for finer details of the vibration dynamics to be captured. The consequent improvement in the feedback response (Fig. 6c), achieved through numerical processing of the frequency-modulated SMI signal, exemplifies the benefits accrued from this modulation approach. The enhanced output signal exhibits a higher signal-to-noise ratio and improved fidelity, enabling more precise extraction of vibration characteristics compared to the unmodulated case.

To evaluate the efficacy of our FM-SMI system in detecting small-amplitude vibrations, we conducted experiments targeting the oscillations of a speaker exhibiting reduced displacement amplitudes. Figure 7 presents the feedback signals obtained from our FM-SMI apparatus under these low-amplitude vibration conditions. In contrast to the unmodulated SMI signals depicted in Fig. 4, which exhibited greater fluctuations and instabilities, the FM-SMI signals displayed remarkable stability and consistency, even for these minute vibration magnitudes. The results showed in Fig. 7 provide compelling evidence of the advantages offered by our FM-SMI approach, particularly when investigating small-amplitude vibrations. While the unmodulated SMI signals (Fig. 4) exhibited substantial variations and instabilities, the frequency-modulated counterparts demonstrated exceptional signal stability and robustness, even in the low-amplitude vibration regime. This enhanced signal quality and stability can be attributed to the inherent properties of frequency modulation. By intentionally modulating the laser frequency, we effectively subdivide the interference patterns into higher-resolution components, mitigating the impact of noise and interference effects that typically plague unmodulated SMI setups.
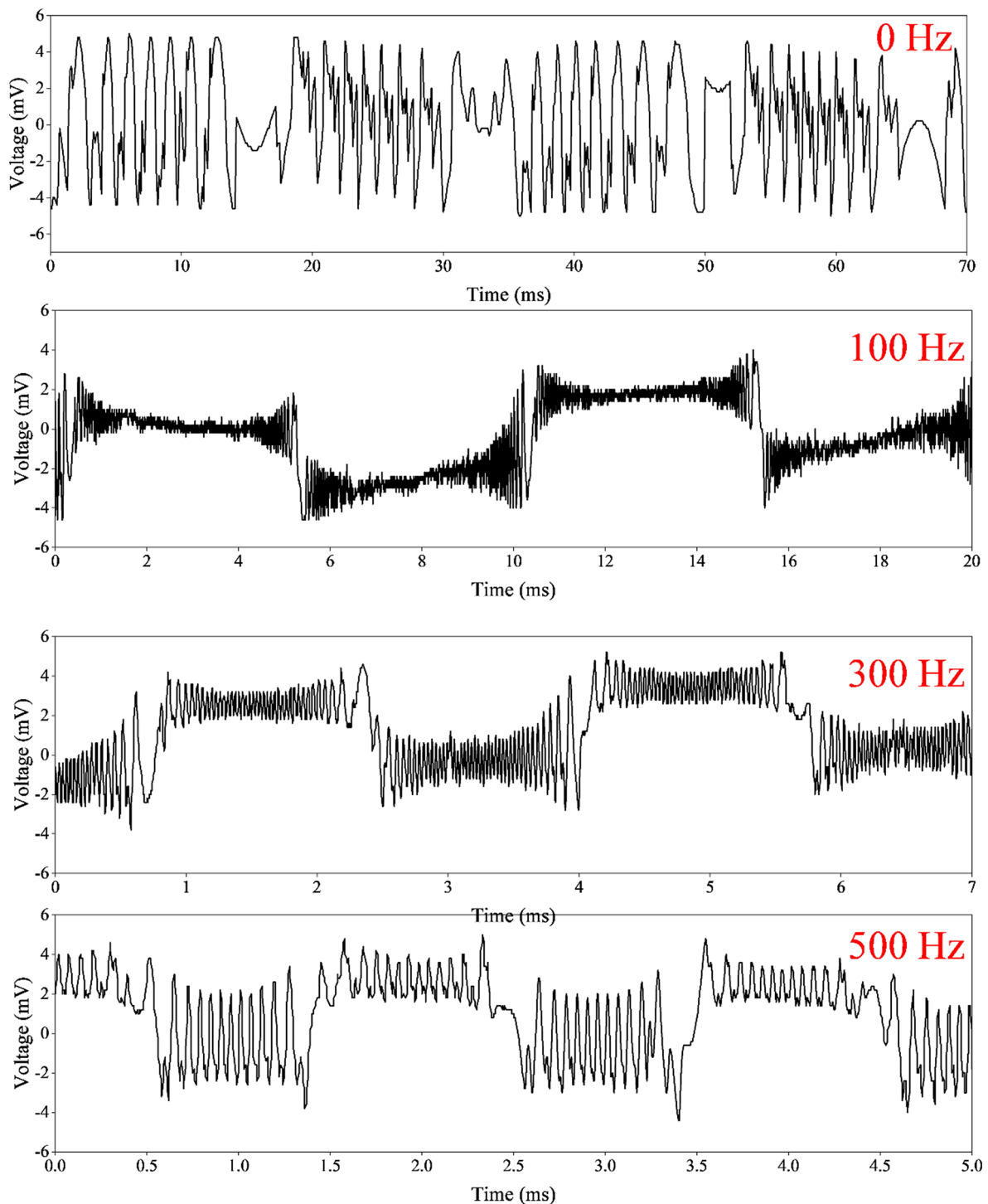
Fig. 5 Measured displacements corresponding to small-amplitude vibrations of the speaker, detected by the self-mixing interference setup. A functional generator was employed to produce sinusoidal waveforms at varying frequencies, facilitating the systematic exploration of the system's detection capabilities in the low-amplitude regime

To demonstrate the practical applicability of our FM-SMI system, we targeted a spin coater, a commonly used apparatus in experimental fabrication processes. A silicon wafer was placed on the spin coater, and we investigated the surface dynamics under two distinct rotational speeds, simulating the topographical variations that arise due to centrifugal forces. Figure 8 presents a comparative analysis of the feedback signals obtained from the unmodulated and frequency-modulated laser beams incident on the spinning wafer. Unlike the previous experiments with a
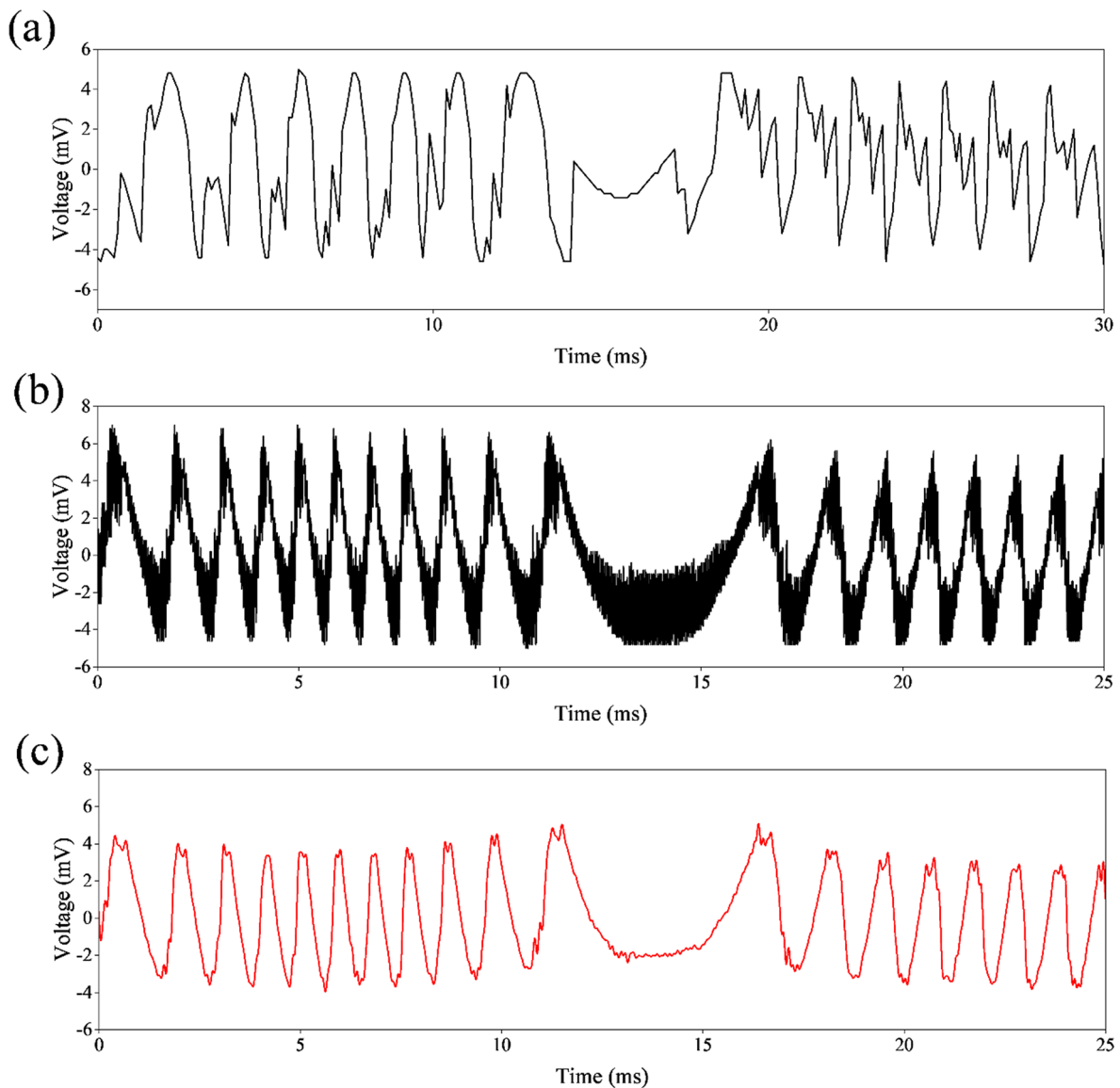
Fig. 6 Comparative analysis of the self-mixing interference signals obtained with (**a**) the unmodulated laser beam and (**b**) the frequency-modulated laser beam at 20 kHz. The frequency modulation induces a segmentation of the interference pattern, increasing the signal resolution. (**c**) The enhanced feedback response extracted from the frequency-modulated signal through numerical processing techniques

mirror-coated speaker (90% reflectivity), the silicon wafer exhibited a lower reflectivity of approximately 30%. Consequently, the unmodulated SMI signal showed a substantial reduction in intensity. However, the FM-SMI approach yielded a signal that, consistent with previous observations, exhibited a segmented structure with improved resolution, facilitating the detection of finer surface undulations. The spin coater experiments, as depicted in Fig. 8, serve as a compelling demonstration of the FM-SMI technique's practical utility in real-world scenarios. Despite the lower reflectivity of the silicon wafer compared to the mirror-coated speaker, our FM-SMI system could effectively capture the surface dynamics under varying rotational speeds. The diminished intensity of the unmodulated SMI signal highlights the challenges associated with low-reflectivity targets, which can lead to reduced signal-to-noise ratios and compromised measurement accuracy. However, the FM-SMI approach circumvented this limitation by enhancing the signal resolution through frequency modulation, effectively subdividing the interference patterns into higher-resolution components. This ability to resolve finer details, even in the presence of lower reflectivity targets, underscores the robustness and versatility of our FM-SMI technique. It enables precise characterization of surface topographies and vibration dynamics across a diverse range of materials and experimental conditions, extending its applicability beyond highly reflective surfaces. The practical relevance of this spin coater investigation lies in its direct connection to
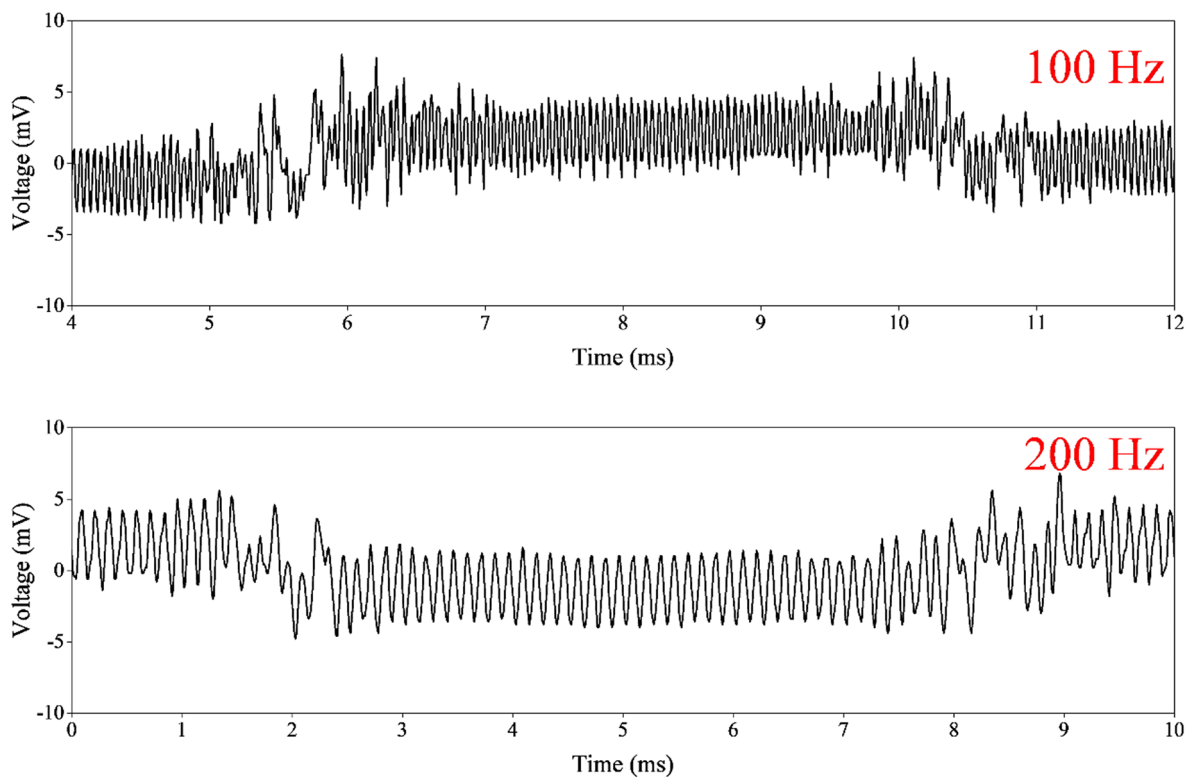
Fig. 7 Feedback signals obtained from the FM-SMI system under low-amplitude vibration conditions of the speaker. In contrast to the unmodulated signals, the FM-SMI signals exhibit higher stability and consistency, highlighting the advantages of the proposed approach

manufacturing processes involving wafer handling and processing. The capability to monitor surface undulations and irregularities during rotation can provide invaluable insights into process optimization, defect detection, and quality control measures, ultimately contributing to improved manufacturing yields and product reliability.

Figure 9 presents the FM-SMI signals obtained from the spinning silicon wafer under two distinct rotational speeds of the spin coater. At 500 rpm (Fig. 9a), the periodic variation in the FM-SMI signal corresponds to a frequency of 5 Hz (120 ms period), consistent with the expected frequency induced by the spin coater's rotation. The interference fringes within the signal provide insights into the minute amplitude variations associated with the wafer's surface dynamics. When the spin coater's rotational speed was increased to 1943 rpm (Fig. 9b), the FM-SMI signal exhibited a periodic modulation at 32.38 Hz (30.8 ms period), accurately tracking the higher rotational frequency. Once again, the interference fringes embedded within the signal serve as indicators of the evolving amplitude changes, enabling the estimation of the wafer's surface undulations.

In a previous study, researchers employed a servo-motor-driven rotational setup as the target and utilized the SMI technique to measure the rotational speed [37]. They found that to acquire a satisfactory signal, several parameters needed to be optimized, such as the distance between the sensor head and the motor shaft, amplifier noise, and lens focal position. The SMI signal was obtained by tracing the minuscule variations in optical power with the built-in PD. However, a major challenge faced by this system was the substantial interference introduced by the servo motor itself, severely degrading the quality of the SMI signal. The rough surface of the motor shaft caused a speckle effect on the coherent laser light reflected from the laser diode, resulting in random amplitude fluctuations, distortion of the ideal waveform, and spectral broadening, ultimately affecting the measurement accuracy. In contrast, our proposed FM-SMI technique exhibits remarkable advantages. By modulating the laser frequency, the FM-SMI system effectively segments the interference signal, increasing the temporal resolution and enhancing signal stability and robustness. Even when probing low-amplitude vibrations or low-reflectivity targets, the FM-SMI system maintains superior performance. Furthermore, the FM-SMI technique possesses noise-suppression capabilities, mitigating the impact of environmental interference and the speckle effect arising from rough target surfaces to a certain extent. Our experimental results indicate that the FM-SMI system can accurately capture surface dynamics in practical applications, such as rotating silicon wafers, providing valuable insights for process optimization and defect detection.
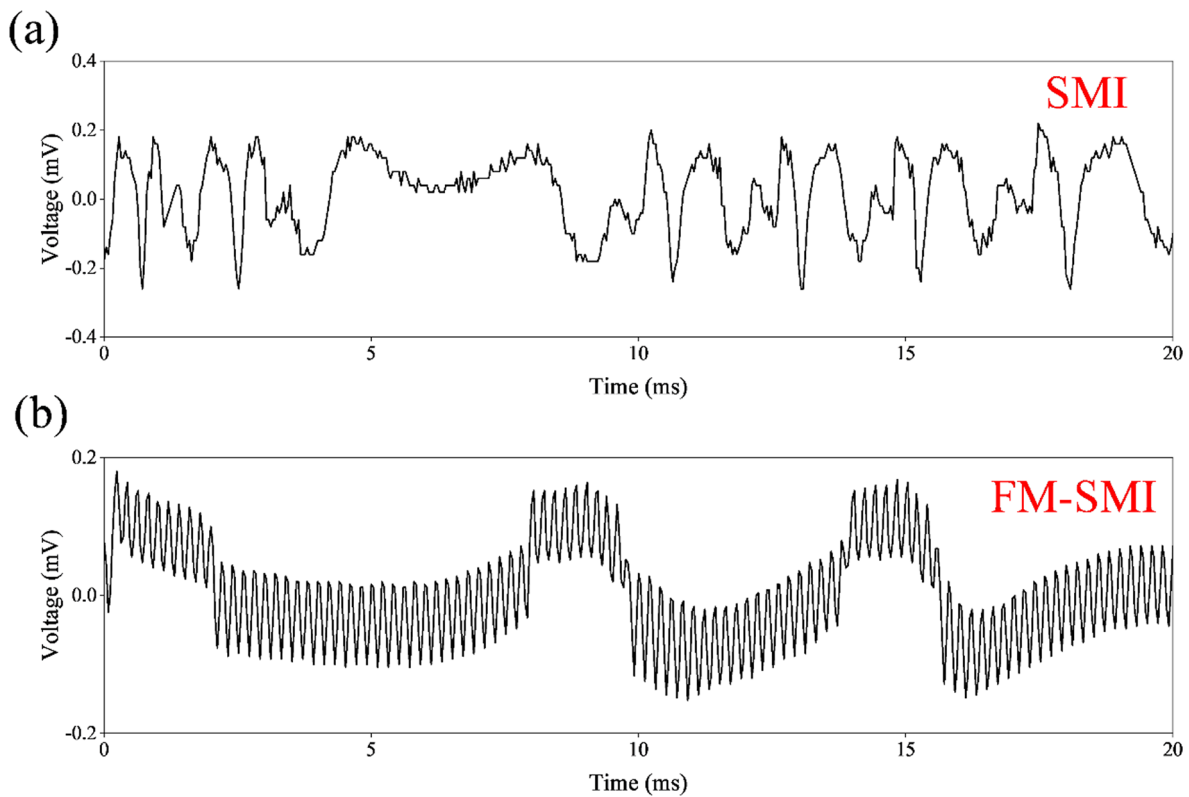
(a)

(b)

Fig. 8 Comparative analysis of the feedback signals obtained from (**a**) the unmodulated laser beam and (**b**) the frequency-modulated laser beam incident on a rotating silicon wafer mounted on a spin coater. The FM-SMI approach yields a segmented signal structure with improved resolution, facilitating the detection of surface undulations despite the lower reflectivity of the silicon wafer

We further investigated the impact of FM on displacement measurements in SMI through theoretical analysis and numerical simulation [32, 38]. The displacement (ΔL) calculated from the frequency modulation (Δf) is given by

$$\Delta L = \left(\frac{\lambda_0}{4\pi n}\right) \times \arctan$$

$$\left[\frac{-J_{2k} \times (2\pi\Delta f L n)}{c} \times \frac{I_{(2k-1)\omega}}{\left(\frac{J_{2k-1} \times (2\pi\Delta f L n)}{c} \times I_{(2k)\omega}\right)}\right] \qquad (6)$$

where ΔL is the measured displacement, λ_0 is the central wavelength of the laser, n is the refractive index of the medium, Δf is the frequency modulation range, L is the external cavity length, c is the speed of light, J_{2k} and J_{2k-1} are Bessel functions of the first kind, and $I_{(2k-1)\omega}$ and $I_{2k\omega}$ represent the intensities of the (2k-1)th and 2kth harmonic components of the SMI signal, respectively. We simulated the variation of DL across a frequency modulation range of 0 to 1000 MHz, as shown in Fig. 10. The results reveal a significant influence of frequency modulation on SMI displacement measurements. In the low-frequency modulation range (approximately 0-200 MHz), ΔL exhibits rapid changes with increasing Δf, indicating high measurement

sensitivity in this region. As the modulation frequency further increases, particularly in the 200–600 MHz range, the rate of change in ΔL becomes more gradual. Notably, the ΔL-Δf curve displays quasi-periodic variations, closely related to the characteristics of Bessel functions. This periodicity suggests the existence of optimal frequency modulation values for system performance. These findings have important implications for practical SMI applications. The varying system behavior across different frequency modulation ranges provides a theoretical foundation for optimizing SMI measurement strategies. For instance, high-precision measurements may benefit from selecting Δf ranges where ΔL is most sensitive to changes, while broader, less precise measurements might utilize ranges where ΔL varies more gradually. However, this non-linear relationship also presents challenges. In practical applications, a trade-off between measurement sensitivity and system stability is necessary. While high-sensitivity regions facilitate precise measurements, they may also be more susceptible to environmental disturbances. Consequently, selecting an appropriate frequency modulation range becomes crucial in optimizing SMI system performance.
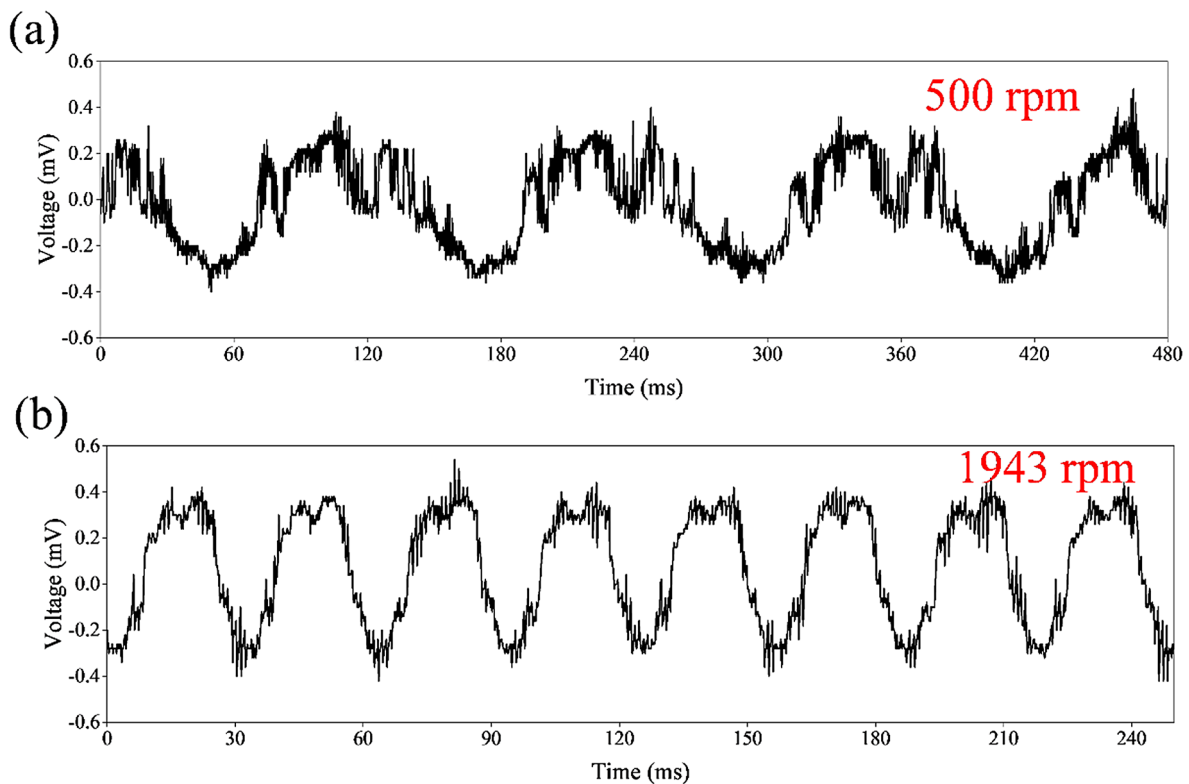
(a)

(b)

Fig. 9 FM-SMI signals obtained from the spinning silicon wafer at (**a**) 500 rpm and (**b**) 1943 rpm rotational speeds of the spin coater. The periodic modulations in the signals accurately track the respective rotational frequencies, while the interference fringes provide insights into the associated amplitude variations and surface dynamics
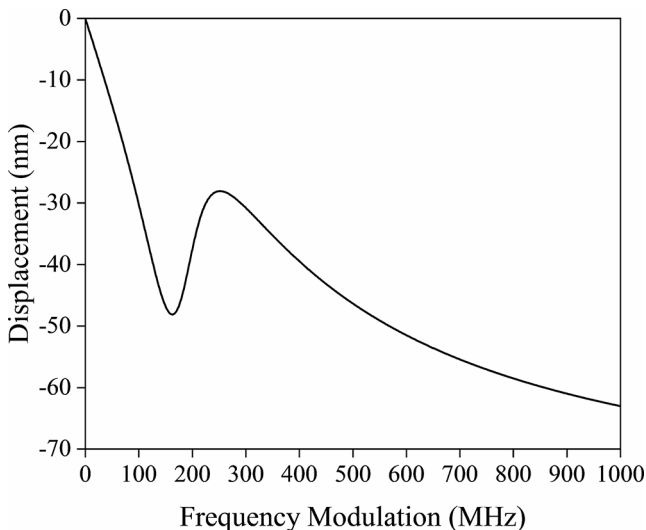

Fig. 10 Relationship between displacement and frequency modulation in a SMI system. The graph shows the calculated displacement (nm) as a function of frequency modulation (MHz) over a range of 0 to 1000 MHz. The non-linear response illustrates the complex influence of frequency modulation on SMI displacement measurements, with notable features including a rapid initial decrease, a local minimum around 150 MHz, and a subsequent gradual decline in displacement magnitude

4 Conclusions

In this work, we have successfully demonstrated a frequency modulation approach, FM-SMI, that significantly enhances the capabilities of self-mixing interference systems for vibration sensing applications. By modulating the laser frequency up to 20 kHz, the FM-SMI technique induces a segmentation of the interference signal, effectively increasing the temporal resolution and enabling the detection of finer vibration details. Through comprehensive experimental investigations involving oscillating speakers and rotating silicon wafers, we have validated the superior performance of the FM-SMI system compared to conventional unmodulated SMI setups. The frequency-modulated signals exhibited exceptional stability and robustness, even when probing low-amplitude vibrations or targeting low-reflectivity surfaces, surpassing the limitations often encountered in traditional SMI systems. The enhanced signal quality, facilitated by the FM-SMI approach, coupled with numerical processing techniques, enabled precise extraction of vibration characteristics, including amplitude variations and surface topographies. The practical applicability of the FM-SMI technique was demonstrated through experiments involving a spin coater, a commonly used apparatus in semiconductor manufacturing processes. The

ability to accurately monitor surface dynamics and irregularities during wafer rotation holds immense potential for process optimization, defect detection, and quality control measures, ultimately contributing to improved manufacturing yields and product reliability. The versatility of the FM-SMI approach extends beyond the semiconductor industry, opening avenues for its application in various fields where non-contact, high-precision vibration measurements are critical, such as non-destructive testing and the characterization of micro-scale devices. The proposed FM-SMI technique represents a significant advancement in the field of self-mixing interference, offering a powerful and robust solution for high-resolution vibration sensing and surface characterization across a diverse range of materials, experimental conditions, and real-world scenarios.

Author contributions J.-R.L and J.R.L performed the experiments and analyzed the data, and V.K.S.H wrote the main manuscript text and guided the whole experiments. All authors reviewed the manuscript.

Data availability No datasets were generated or analysed during the current study.

Declarations

Competing interests The authors declare no competing interests.

References

1. T. Taimre, M. Nikolić, K. Bertling, Y.L. Lim, T. Bosch, A.D. Rakić, Adv. Opt. Photon. **7**, 570 (2015)
2. J. Li, H. Niu, Y. Niu, Opt. Eng. **56**, 050901 (2017)
3. A.D. Rakić, T. Taimre, K. Bertling, Y.L. Lim, P. Dean, A. Valavanis, D. Indjin, Appl. Phys. Rev. **6**, 021320 (2019)
4. J. Smetana, R. Walters, S. Bauchinger, A.S. Ubhi, S. Cooper, D. Hoyland, D. Martynov, Phys. Rev. Appl. **18**, 034040 (2022)
5. S. Yang, G. Zhang, Meas. Sci. Technol. **29**, 102001 (2018)
6. A.M. Pérez, G. Rodríguez-Zurita, V.H. Flores-Muñoz, G. Parra-Escamilla, D.I. Serrano-García, A. Martínez-García, N.I. Toto-Arellano: Opt. Rev. 26, 231 (2019)
7. G. Giuliani, M. Norgia, S. Donati, T. Bosch, J. Opt. A: Pure Appl. Opt. **4**, S283 (2002)
8. S. Donati, Laser Photonics Rev. **6**, 393 (2012)
9. T. Taimre, M. Nikolić, K. Bertling, Y.L. Lim, T. Bosch, A.D. Rakić, Adv. Opt. Photonics. **7**, 570 (2015)
10. S. Donati, M. Norgia, Opt. Eng. **57**, 051506 (2018)
11. H. Hao, H. Lin, J. Chen, W. Xia, D. Guo, M. Wang, Opt. Laser Technol. **135**, 106666 (2021)
12. S. Donati, Vibration. **6**, 625 (2023)
13. W.M. Wang, W.J.O. Boyle, K.T.V. Grattan, A.W. Palmer, Appl. Opt. **32**, 1551 (1993)
14. G. Giuliani, S. Bozzi-Pietra, S. Donati, Meas. Sci. Technol. **14**, 24 (2002)
15. L. Scalise, Y. Yu, G. Giuliani, G. Plantier, T. Bosch, IEEE Trans. Instrum. Meas. **53**, 223 (2004)
16. G. Mourat, N. Servagent, T. Bosch, Opt. Eng. **39**, 738 (2000)
17. Y. Zhao, L. Lu, Z. Du, B. Yang, W. Zhang, J. Zhou, B Yu: Optik. **124**, 4707 (2013)
18. C. Jiang, Z. Zhang, C. Li, Opt. Commun. **367**, 227 (2016)
19. C. Zakian, M. Dickinson, T. King, J. Opt. A: Pure Appl. Opt. **7**, S445 (2005)
20. C. Zakian, M. Dickinson, T. King, Appl. Opt. **45**, 2240 (2006)
21. V. Contreras, J. Lönnqvist, J. Toivonen, Opt. Express. **24**, 8886 (2016)
22. A. Magnani, D. Melchionni, A. Pesatori, M. Norgia, Opt. Commun. **365**, 133 (2016)
23. C. Chen, Y. Zhang, X. Wang, X. Wang, W. Huang, IEEE Photonics J. **7**, 1 (2015)
24. S. Donadello, A.G. Demir, B. Previtali, Appl. Opt. **57**, 7232 (2018)
25. B. Wang, B. Liu, L. An, P. Tang, H. Ji, Y Mao: Photonics. **8**, 550 (2021)
26. B. Liu, B. Wang, Y. Ruan, Y. Yu, J. Xi, H. Ji, P. Tang, Opt. Laser Technol. **176**, 110963 (2024)
27. E. Fischer, E. Dalhoff, S. Heim, U. Hofbauer, H.J. Tiziani, Appl. Opt. **34**, 5589 (1995)
28. V.S. Sobolev, G.A. Kashcheeva, Optoelectron. Instrum. Data Process. **44**, 519 (2008)
29. M. Norgia, D. Melchionni, S. Donati, IEEE Photonics Technol. Lett. **29**, 1552 (2017)
30. M. Norgia, F. Bandi, A. Pesatori, S. Donati, J. Phys.: Conf. Ser. **1249**, 012020 (2019)
31. T.T. Vu, H.H. Hoang, T.T. Vu, N.T. Bui, Appl. Sci. **10**, 2693 (2020)
32. S. Donati, M. Norgia, IEEE J. Quantum Electron. **53**, 1 (2017)
33. V. Contreras, H. Martinez, M. Norgia, IEEE Photonics Technol. Lett. **30**, 1909 (2018)
34. D. Guo, Z. Xie, Q. Yang, W. Xia, Y. Yu, M. Wang, Photonics. **10**, 839 (2023)
35. B. Liu, Y. Ruan, Y. Yu, J. Lightwave Technol. **39**, 4062–4068 (2021)
36. L. An, B. Liu, Opt. Express. **30**(11), 19134–19144 (2022)
37. H. Sun, J.G. Liu, Q. Zhang, R. Kennel, Appl. Opt. **55**, 236 (2016)
38. T.T. Vu, M. Higuchi, M. Aketagawa, Meas. Sci. Technol. **27**, 105201 (2016)